Analytical model of high-frequency resonant tunneling: The first-order ac current response

H. C. Liu
Institute for Microstructural Sciences, National Research Council, Ottawa, Canada K1A 0R6

(Received 25 July 1990; revised manuscript received 8 February 1991)

A high-frequency analytical model for double-barrier resonant tunneling is formulated. In evaluating the device frequency response, a dc voltage is applied to bias the double barrier into the resonant-tunneling regime, and a small-amplitude ac modulation is then added. The ac modulation causes transmission sidebands, in addition to the direct transmission peak when an electron traverses the double barrier. Analytical expressions for the first-order sidebands are derived. Using a Breit-Wigner expansion of the sidebands in the neighborhood of a resonance, the small-signal ac current response is evaluated in *closed* form. The device frequency characteristic is discussed, and a quantum inductance is confirmed, which arises from the resonance lifetime. An analytical model is useful in understanding the device physics and in applications.

I. INTRODUCTION

High-frequency device applications are doubtless the major driving forces for studying heterojunction double-barrier resonant-tunneling (RT) devices. Experiments ranging from detectors up to 2.5 THz (Ref. 1) and quantum-well oscillators up to 420 GHz (Refs. 2–5) to fabrications of RT transistors[6,7] as well as experimental studies of equivalent circuits[8] employing $Al_xGa_{1-x}As$-GaAs structures have been carried out. Important studies in understanding physical processes have been reported.[9–11] Calculations of tunneling currents under both dc and ac voltages have been undertaken.[12–15] Several authors have carried out self-consistent analyses of dc current-voltage (I-V) characteristics.[16–18] Theoretical considerations of device frequency limits have been addressed in a number of papers.[3,4,19–21] In most previous works, the device intrinsic response is assumed to be related to the tunneling time, and hence the frequency limit is proportional to the inverse of this time. Frensley has used an alternative approach in which the Wigner function distributions of the time-dependent quantum-mechanical system have been solved numerically.[22,23] Yet another approach using the Kubo formula to calculate the frequency dependence has been presented.[24]

In this paper we formulate an analytical model for high-frequency double-barrier RT devices. A numerical technique and general properties of scattering matrices have been given by Coon and Liu[14,15] which are extensions of the standard scattering model.[12,13] The merit of the present work is that it can be evaluated in a *closed analytical* form, and the physical picture is therefore clear. Such a model is extremely useful in understanding the device high-frequency characteristics, and extremely desirable in experiments such as those performed by Brown, Sollner, and co-workers.[2–5]

Our model is shown schematically in Fig. 1. A double-barrier structure is biased with both dc and ac voltages resulting in potential energies across the double barrier V_{dc} and $V_{ac}\cos\omega t$, respectively. The potentials are linearly distributed across the double barrier from $V_{dc} = V_{ac} = 0$ in the emitter to constant values $-V_{dc}$ and $-V_{ac}$ in the collector. Since we have chosen the emitter band edge as the energy reference, we have added explicitly the minus signs so that V_{dc} and V_{ac} are non-negative. These potentials do not include the possible potential distributions in the emitter accumulation layer and the collector depletion region. To consider the small signal ac response we keep the amplitude of the ac potential (V_{ac}) small. We neglect the electrostatic charge effect in the quantum well.[9,16–18] The electron direct tunneling with-

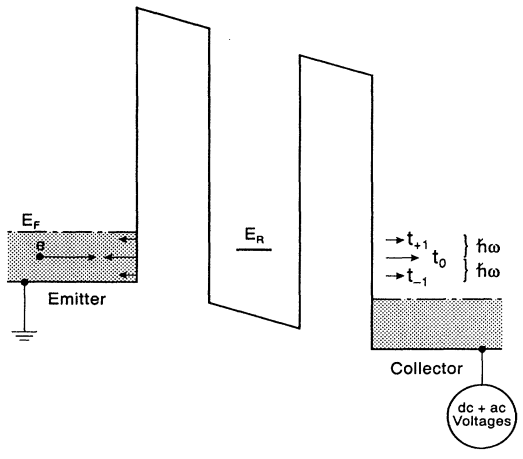

FIG. 1. Double-barrier potential profile under a dc bias and a small amplitude ac modulation. The resonant state is labeled by E_R.

out emission or absorption of energy from the ac field is characterized by the direct transmission amplitude (t_0). The first-order transmission sidebands represent an incident electron absorbing (t_{+1}) or emitting (t_{-1}) an ac modulation quantum ($\hbar\omega$) emerging with a higher ($+\hbar\omega$) or a lower ($-\hbar\omega$) energy. Arrows in Fig. 1 indicate an electron (e) incident from the left (the emitter), the direct transmission (t_0) and the two first-order sidebands ($t_{\pm1}$) to the right (the collector), and the reflections to the left. We neglect higher-order terms, e.g., the second-order sidebands $t_{\pm2}$ and so on. The first-order transmission sidebands have been used in discussing the tunneling traversal time for a single barrier.[25]

We hope to derive an analytical expression for the first-order sidebands similar to the Breit-Wigner form for the direct tunneling:

$$t_0 \propto \frac{i\Gamma}{E - E_R + i\Gamma}, \tag{1}$$

where E_R is the resonance energy and Γ is the resonance width, since it is known that an analytical tunneling current expression can be obtained for the dc case using the Breit-Wigner form.[20] Intuitively, one might expect that the sidebands $t_{\pm1}$ should have resonance Breit-Wigner line shapes but peaked at E_R and $E_R \mp \hbar\omega$, respectively,

$$t_{\pm1} \propto \frac{i\Gamma}{E - E_R + i\Gamma} \frac{i\Gamma}{E - E_R \pm \hbar\omega + i\Gamma}, \tag{2}$$

because $t_{\pm1}$ are associated with absorption and emission assisted tunneling processes involving an ac modulation quantum $\hbar\omega$. We will see later in Sec. II that $t_{\pm1}$ indeed have the features displayed in Eq. (2).

The paper is organized in the following way. Section II gives the analytical results of the transmission amplitudes for the first-order sidebands ($t_{\pm1}$). For completeness, some details[14,15] in arriving at the starting point of the the present paper are reviewed in Appendix A. Because of the lengthy algebra the derivations for the transmission amplitudes are given in Appendixes B and C. Section III presents the details of the calculated current response and this section contains the main results of this paper. Section IV discusses the efficiency of photon emission into the ac field which is relevant to the oscillator experiments.[2-5] Finally, Sec. V gives the concluding remarks.

II. RESONANT TRANSMISSION AMPLITUDES

We use a coherent scattering approach which extends the standard model for the dc case.[12,13] The incident plane wave in the emitter region is

$$\psi_{\text{in}} = e^{ikz - iEt/\hbar}, \tag{3}$$

where k is the wave vector related to the energy by $E = \hbar^2k^2/2m$, m is the effective mass, the tunneling direction is chosen as the z coordinate, and the $z = 0$ plane is chosen to coincide with the heterointerface between the emitter contact and the emitter barrier. Note that the energy reference and the potential ground are at the band edge of the emitter as shown in Fig. 1. We assume that the effective mass is constant throughout the structure. One can view this simplification as a model which enables us to derive the following analytical result. A position-dependent effective mass destroys the simple one-dimensional nature of the problem, i.e., dimensions perpendicular to the current can no longer be incorporated by simply including a proper density of states. In a constant potential region and in the presence of a constant amplitude ac modulation, one can still find a plane-wave solution to the time-*dependent* Schrödinger equation, which we use as bases.[14,15] The transmitted wave in the collector side (including up to first-order sidebands) is

$$\psi_{\text{tran}} = (t_0 e^{ik_0 z} + t_{+1} e^{ik_{+1} z - i\omega t} + t_{-1} e^{ik_{-1} z + i\omega t}) e^{-iEt/\hbar} U, \tag{4}$$

where $U = \exp[iV_{\text{ac}} \sin(\omega t)/\hbar\omega]$ is a phase factor due to the constant amplitude ac modulation,[14,15] the $z = 0$ plane has been moved to the heterointerface between the collector contact and the collector barrier, k_0 and $k_{\pm1}$ are wave vectors for energies E and $E \pm \hbar\omega$ in the collector region. The mathematical details in arriving at Eq. (4) have been given before,[14,15] and for completeness we briefly review the important steps in Appendix A. Note that the potential energy in the collector is $-V_{\text{dc}} - V_{\text{ac}} \cos\omega t$. The wave function in Eq. (4) can be easily verified to satisfy the time-dependent Schrödinger equation with a constant amplitude ac potential. In fact, each individual term together with $e^{-iEt/\hbar}U$ is a plane-wave solution to the time-dependent Schrödinger equation. We consider the case where only the emitter electrons contribute to the tunneling current since this is the case relevant to most of the practical devices. Electrons from the collector cannot be neglected when, e.g., the resonant energy is low such that $E_R < E_F$. Physically, Eqs. (3) and (4) describe a multichannel scattering state with plane wave incident from the emitter, and direct tunneling and first-order sidebands outgoing plane waves in the collector (see Fig. 1). We have omitted writing down the reflected waves back to the emitter explicitly.

Within the first-order approximation, where t_0 is the same as for the case of $V_{\text{ac}} = 0$ and $t_{\pm1}$ is proportional to the first order in V_{ac}, the transmission amplitudes can be evaluated analytically. The Breit-Wigner form for t_0 is well known and the derivation is given in Appendix B for completeness and for detail that will be used in deriving $t_{\pm1}$. In the neighborhood of a resonance, the transmission coefficient defined as the ratio of the transmitted and the incident currents, and the phase (ϕ_0) of t_0 are given by

$$T_0 \approx T_{0,\max} \frac{\Gamma^2}{(E - E_R)^2 + \Gamma^2}, \tag{5}$$

$$\phi_0 \approx \phi_{00} + \tan^{-1} \frac{E - E_R}{\Gamma}, \tag{6}$$

where the on-resonance transmission coefficient $T_{0,\max} = 4T_E T_C/(T_E + T_C)^2$, $T_{E/C}$ is the transmission coefficient for the emitter or collector barrier evaluated at the resonance energy, and ϕ_{00} has a weak (nonresonant) energy dependence. It is interesting to point out that $T_{0,\max}$ vanishes when E_R coincides with the emitter band edge because in this case the incident electron kinetic energy approaches zero so that $T_E \to 0$. This, for some devices where the bottom of the emitter Fermi sea is at the band edge (e.g., in the case where the accumulation effect is negligible for a heavily doped emitter), leads to an unfavorable increase in the magnitude of the negative differential resistance (NDR) because the NDR region corresponds to the resonant state approaching the bottom of the emitter Fermi sea and $T_{0,\max}$ decreases with increasing bias. This will degrade the steepness of the NDR region which was neglected in our early model.[20] However, when the bottom of the emitter Fermi sea is at a finite energy (e.g., in the case where the accumulation leads to quasi-one-dimensional states in the emitter for a lightly doped emitter or with an undoped buffer layer inserted before the double barrier), $T_{0,\max}$ changes slowly with E_R and within the voltage range where RT occurs $T_{0,\max}$ can be taken as a constant. In this case, the magnitude of the NDR directly reflects the size of the resonance width Γ.

The first-order absorption and emission processes can also be expressed analytically in a similar way. We give the details of the derivation of $t_{\pm 1}$ in Appendix C and the result is

$$T_{\pm 1} \approx \left(\frac{V_{\rm ac}}{2\hbar\omega}\right)^2 T_{0,\max} \times \frac{\Gamma^2[(E - E_R \pm \hbar\omega/2)^2 + \Gamma^2]}{[(E - E_R)^2 + \Gamma^2][(E - E_R \pm \hbar\omega)^2 + \Gamma^2]}, \quad (7)$$

$$\phi_{\pm 1} \approx \phi_{\pm 1,0} + \tan^{-1}\frac{E - E_R}{\Gamma} - \tan^{-1}\frac{E - E_R \pm \hbar\omega/2}{\Gamma} + \tan^{-1}\frac{E - E_R \pm \hbar\omega}{\Gamma}, \quad (8)$$

where $\phi_{+1,0} \approx \phi_{00}$ and $\phi_{-1,0} \approx \phi_{00} + \pi$. As we will see in Sec. III, the information about the phases of the transmission amplitudes is important when one considers the ac current which arises from bilinear terms like $t_0 t^*_{\pm 1}$ as the leading order. The analytical result for $T_{\pm 1}$ given in Eq. (7) is valid for $V_{\rm ac}/\hbar\omega < 1$ because of the expansion that we have made (see Appendix C), and hence it is naturally suited for evaluating the device small signal response. Equation (7) displays a double peaked structure with transmission enhanced at $E = E_R$ and $E = E_R \mp \hbar\omega$. Physically, this is easy to understand because $t_{\pm 1}$ describes one photon assisted resonant tunneling. Figure 2 shows the two favored absorption processes (t_{+1}) for incident energies E_R and $E_R - \hbar\omega$, respectively. The two processes both have the resonant state as the intermediate state and hence they are enhanced in comparison with processes at other energies. The upward arrows span both well and barriers indicating that the absorption can occur anywhere in the well or the barriers. The analytical formalism was compared with numerical results using the method given by Coon and Liu[14] and by Liu,[26] and a good agreement was found.

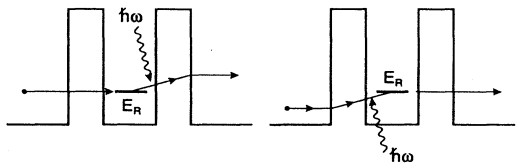

FIG. 2. Two favored energies (left, $E = E_R$ and right, $E = E_R - \hbar\omega$) for the absorption transmission sideband t_{+1}.

III. RESONANT TUNNELING CURRENTS

In this section we use the expressions given in Sec. II to discuss the small signal ac current response. Because the expressions in Sec. II are valid only in the neighborhood of a resonance, the currents that we calculate in this section are associated with a resonance, i.e., we consider only resonant tunneling currents. The single electron tunneling current

$$j = (e\hbar/2im)\left(\psi^*_{\rm tran}\frac{d\psi_{\rm tran}}{dz} - \psi_{\rm tran}\frac{d\psi^*_{\rm tran}}{dz}\right) \quad (9)$$

is evaluated in the collector side using Eq. (4) and setting $z = 0$:

$$j = \frac{e\hbar k_0}{m}|t_0|^2 + \frac{e\hbar}{m}\,{\rm Im}[ik_0 t_0(t^*_{+1}e^{i\omega t} + t^*_{-1}e^{-i\omega t}) + it^*_0(k_{+1}t_{+1}e^{-i\omega t} + k_{-1}t_{-1}e^{i\omega t})], \quad (10)$$

where Im[$\cdots$] means taking the imaginary part and terms bilinear in $t_{\pm 1}$ are omitted. Since $\hbar^2 k_0^2/2m = E + V_{\rm dc}$ and $\hbar^2 k^2_{\pm 1}/2m = E + V_{\rm dc} \pm \hbar\omega$, and $V_{\rm dc}$ is normally much larger than $\hbar\omega$, $k_0 \approx k_{\pm 1}$ is a good approximation. Note that E is referenced with respect to the emitter band edge. Equation (10) becomes

$$\begin{aligned} j &= j_{\rm dc} + j_{\rm ac}, \\ j_{\rm dc} &\equiv (e\hbar k_0/m)|t_0|^2, \\ j_{\rm ac} &\equiv (2e\hbar k_0/m)\,{\rm Re}[t_0(t^*_{+1}e^{i\omega t} + t^*_{-1}e^{-i\omega t})], \end{aligned} \quad (11)$$

where Re[$\cdots$] means taking the real part. Because the first term in Eq. (10) gives rise to the usual dc tunneling current, and the rest is the leading-order ac current response, we have separated j into $j_{\rm dc} + j_{\rm ac}$. Classically (in the low-frequency limit), the ac current response should reduce to the differential conductance multiplied by the ac voltage as we will see later. In general, the ac current response would have an arbitrary phase relationship with respect to the applied potential $V_{\rm ac}\cos\omega t$.

To investigate to what extent currents in the emitter and the collector are conserved, we use the following continuity equation derived from the time-dependent

Schrödinger equation:

$$j^{(E)} - j^{(C)} = e\frac{\partial}{\partial t}\int_{\mathrm{DB}} \psi^*\psi\, dz, \tag{12}$$

where $j^{(E/C)}$ is the instantaneous current density in the emitter or collector, $j^{(C)}$ is the j given in Eqs. (9)–(11) for an electron incident from the emitter, the integration on the right-hand side is over the double-barrier (DB) region. To calculate $j^{(E)}$, we must include the reflected waves described by the reflection amplitudes r_0, $r_{\pm 1}$, and so on. The first-order reflection sideband amplitudes ($r_{\pm 1}$) are proportional to $V_{\mathrm{ac}}/\hbar\omega$, and analytical expressions for $r_{\pm 1}$ can be obtained using a similar derivation given in Appendix C. Using the time-dependent wave function $\psi_{\mathrm{in}} + \psi_{\mathrm{refl}}$ in the emitter, we can separate the current $j^{(E)}$ into incident $j_{\mathrm{in}}^{(E)}$ and reflected $j_{\mathrm{refl}}^{(E)}$ parts. The incident current is independent of time, while similar to $j^{(C)}$ in Eq. (11) the reflected current has both time-independent (dc) and time-dependent (ac) parts. From Eq. (12), we have

$$j_{\mathrm{dc}}^{(E)} = j_{\mathrm{dc}}^{(C)}, \tag{13}$$

$$j_{\mathrm{ac}}^{(E)} - j_{\mathrm{ac}}^{(C)} = \frac{\partial}{\partial t} Q_{\mathrm{DB}}, \tag{14}$$

where $Q_{\mathrm{DB}} = e\int_{\mathrm{DB}} \psi^*\psi\, dz$ is the charge in the double-barrier region. Equation (13) shows that the dc part of the current is conserved, i.e., position independent. This is true in general even when all orders of sidebands are included,[14,15] whereas the first-order ac (sinusoidal) part of the current would be different when evaluated at an arbitrary z coordinate. The difference in the instantaneous ac currents between two points is related to the increase of charge in the region defined by the two points as given quantitatively by Eq. (14). We assume that the emitter and the collector layers are heavily doped, therefore the current evaluated at $z = 0$ in the collector is the instantaneous current in the external circuit at the collector lead (and this is the current we will concentrate on in the following calculations). If, on the other hand, a lightly doped or an undoped buffer is employed in the collector, we must evaluate the current at a position where the heavily doped contact layer starts ($z > 0$), and an extra phase delay is found in the ac current, which is associated with the delay of electrons propagating across the buffer layer, as proposed by Sollner *et al.*[3]

Integrating over the emitter Fermi sea we obtain the total current density at $z = 0$ and zero temperature,

$$J = (1/4\pi^2)\int_0^{k_F} dk\,(k_F^2 - k^2)\, j = (m^2/2\pi^2\hbar^4)\int_0^{E_F} dE\,(E_F - E)\, j/k, \tag{15}$$

where k_F is the emitter Fermi wave vector related to the Fermi energy by $E_F = \hbar^2 k_F^2/2m$ and k (the wave vector in the *emitter*) in j/k will be combined with j [given in Eq. (11)] to give the transmission coefficient, e.g., $T_0 = (k_0/k)|t_0|^2$. Note that we consider cases where the collector side does not contribute to the tunneling current, i.e., the bias voltage is large enough to offset emitter and collector Fermi seas ($E_F < V_{\mathrm{dc}}$). Furthermore we neglect many-body Fermion effects which provide no corrections up to the first order. The complete formalism has been given by Coon and Liu.[14,15] Substituting Eq. (11) into (15) and using Eq. (5), the dc part in Eq. (11) results in

$$J_{\mathrm{dc}} = \frac{em}{2\pi^2\hbar^3} T_{0,\max}\int_0^{E_F} dE(E_F - E)\frac{\Gamma^2}{(E - E_R)^2 + \Gamma^2}, \tag{16}$$

which, after integration, becomes

$$J_{\mathrm{dc}} = \frac{em}{2\pi^2\hbar^3} T_{0,\max}\Gamma\left[(E_F - E_R)\left(\tan^{-1}\frac{E_F - E_R}{\Gamma} + \tan^{-1}\frac{E_R}{\Gamma}\right) - \frac{\Gamma}{2}\ln\frac{(E_F - E_R)^2 + \Gamma^2}{E_R^2 + \Gamma^2}\right], \tag{17}$$

where E_R is related to the bias by $E_R = E_{R0} - V_{\mathrm{dc}}/2$ (for a symmetric structure) and E_{R0} is E_R at zero bias. This expression is identical to that for the case where only a dc voltage is applied.[20] We ignore charge redistribution effects[16–18] for simplicity. In reality a non-negligible fraction of the applied voltage is distributed in the emitter accumulation layer and in the collector depletion region. In the narrow resonance limit ($\Gamma \ll E_R$ and $\Gamma \ll E_F - E_R$), Eq. (17) gives a triangular-shaped I-V characteristic:[20]

$$J_{\mathrm{dc}} = \frac{em}{2\pi\hbar^3} T_{0,\max}\Gamma(E_F - E_R)\Theta(E_R)\Theta(E_F - E_R), \tag{18}$$

where $\Theta(\cdots)$ is the usual unity step function.

Substituting t_0 and $t_{\pm 1}$ in Sec. II [Eqs. (5)–(8)] into the (time-dependent) ac part of the current in Eq. (11), we get

$$j_{\mathrm{ac}} = \frac{e\hbar k}{m}\frac{V_{\mathrm{ac}}}{\hbar\omega} T_0\left[\left(\frac{(E - E_R + \hbar\omega/2)^2 + \Gamma^2}{(E - E_R + \hbar\omega)^2 + \Gamma^2}\right)^{1/2}\cos\left(\omega t + \tan^{-1}\frac{E - E_R + \hbar\omega/2}{\Gamma} - \tan^{-1}\frac{E - E_R + \hbar\omega}{\Gamma}\right) - \left(\frac{(E - E_R - \hbar\omega/2)^2 + \Gamma^2}{(E - E_R - \hbar\omega)^2 + \Gamma^2}\right)^{1/2}\cos\left(\omega t - \tan^{-1}\frac{E - E_R - \hbar\omega/2}{\Gamma} + \tan^{-1}\frac{E - E_R - \hbar\omega}{\Gamma}\right)\right]. \tag{19}$$

Using the following

$$\cos(\alpha + \beta + \gamma) = \cos\alpha\cos\beta\cos\gamma - \cos\alpha\sin\beta\sin\gamma - \sin\alpha\cos\beta\sin\gamma - \sin\alpha\sin\beta\cos\gamma,$$

$$\cos[\tan^{-1}(y/x)] = x/\sqrt{x^2 + y^2},\quad \sin[\tan^{-1}(y/x)] = y/\sqrt{x^2 + y^2},$$

and after some algebraic manipulations, Eq. (19) becomes

$$j_{\rm ac}=\frac{e\hbar k}{m}\frac{V_{\rm ac}}{\hbar\omega}T_0\Bigg[\left(\frac{(E-E_R+\hbar\omega/2)(E-E_R+\hbar\omega)+\Gamma^2}{(E-E_R+\hbar\omega)^2+\Gamma^2}-\frac{(E-E_R-\hbar\omega/2)(E-E_R-\hbar\omega)+\Gamma^2}{(E-E_R-\hbar\omega)^2+\Gamma^2}\right)\cos\omega t$$
$$+(\Gamma\hbar\omega/2)\left(\frac{1}{(E-E_R+\hbar\omega)^2+\Gamma^2}-\frac{1}{(E-E_R-\hbar\omega)^2+\Gamma^2}\right)\sin\omega t\Bigg]. \tag{20}$$

Before carrying out the integration over the emitter Fermi sea for the ac part of the current, we first look at the Taylor series expansion in terms of $\hbar\omega$ and keep the leading-order term in $\hbar\omega$. From Eq. (20), we get

$$j_{\rm ac}\approx\frac{e\hbar k}{m}V_{\rm ac}T_0\Bigg(-\frac{E-E_R}{(E-E_R)^2+\Gamma^2}\cos\omega t$$
$$-\frac{2\hbar\omega\Gamma(E-E_R)}{[(E-E_R)^2+\Gamma^2]^2}\sin\omega t\Bigg). \tag{21}$$

Terms neglected are of the form $O((\hbar\omega)^2)V_{\rm ac}\cos\omega t$, $O((\hbar\omega)^3)V_{\rm ac}\sin\omega t$, and so on, where $O(\cdots)$ has the standard meaning as in calculus. We note that

$$T_0\frac{E-E_R}{(E-E_R)^2+\Gamma^2}=\frac{1}{2}\frac{\partial T_0}{\partial E_R}=-\frac{\partial T_0}{\partial V_{\rm dc}},$$
$$T_0\frac{E-E_R}{[(E-E_R)^2+\Gamma^2]^2}=\frac{\Gamma^2}{2}\frac{\partial}{\partial(\Gamma^2)}\left(\frac{1}{\Gamma^2}\frac{\partial T_0}{\partial V_{\rm dc}}\right),$$

then Eq. (21) becomes

$$j_{\rm ac}\approx\frac{\partial j_{\rm dc}}{\partial V_{\rm dc}}V_{\rm ac}\cos\omega t-\hbar\omega\Gamma^3\frac{\partial}{\partial(\Gamma^2)}\left(\frac{1}{\Gamma^2}\frac{\partial j_{\rm dc}}{\partial V_{\rm dc}}\right)V_{\rm ac}\sin\omega t. \tag{22}$$

From the above equation the total current is trivially obtained:

$$J_{\rm ac}\approx\frac{\partial J_{\rm dc}}{\partial V_{\rm dc}}V_{\rm ac}\cos\omega t-\hbar\omega\Gamma^3\frac{\partial}{\partial(\Gamma^2)}\left(\frac{1}{\Gamma^2}\frac{\partial J_{\rm dc}}{\partial V_{\rm dc}}\right)V_{\rm ac}\sin\omega t, \tag{23}$$

where the first term corresponds to the classical low-frequency expression, while the second represents the leading order high-frequency correction. In the narrow resonance limit $\Gamma\ll E_F$, using Eq. (18), Eq. (23) reduces easily to

$$J_{\rm ac}\approx\frac{\partial J_{\rm dc}}{\partial V_{\rm dc}}[V_{\rm ac}\cos\omega t+(\hbar\omega/2\Gamma)V_{\rm ac}\sin\omega t]\tilde{\Theta}$$
$$=\frac{\partial J_{\rm dc}}{\partial V_{\rm dc}}[1+(\hbar\omega/2\Gamma)^2]^{-1/2}\,V_{\rm ac}\cos(\omega t-\alpha)\tilde{\Theta}, \tag{24}$$

where $\tilde{\Theta}\equiv\Theta(E_R)\Theta(E_F-E_R)$ and $\alpha=\tan^{-1}(\hbar\omega/2\Gamma)$. Note that in this limiting case $\partial J_{\rm dc}/\partial V_{\rm dc}$ is a constant within the potential range defined by the two Θ functions. One can see that for $\hbar\omega\ll\Gamma$ the classical current response is obtained. A phase delay of α relative to the applied ac potential is expected consistent with experiments.[4,5,27] The physical reason for the phase delay is easy to understand. Notice that $\hbar/2\Gamma$ is the resonant lifetime τ, and therefore the delay is associated with the finite lifetime of the resonance. As proposed by Brown, Parker, and Sollner,[4] one can incorporate the phase delay effect into the device equivalent circuit by adding a "quantum" inductance $L_{\rm QW}$ in series with the device differential conductance $G=\partial J_{\rm dc}/\partial V_{\rm dc}$. Then we have $\omega L_{\rm QW}G=\hbar\omega/2\Gamma$, i.e., $L_{\rm QW}=\tau/G$.

The total ac current response can be also evaluated when Eq. (20) is substituted into (15). One obtains a long algebraic expression after the integration over the emitter Fermi sea. We separate the current response into the following form:

$$J_{\rm ac}\equiv y_{\rm Re}(V_{\rm ac}/e)\cos\omega t+y_{\rm Im}(V_{\rm ac}/e)\sin\omega t, \tag{25}$$

where $y_{\rm Re}$ and $y_{\rm Im}$ are the real and the imaginary parts of the device admittance, respectively. The form of the above definition is a consequence of the form of the applied ac potential that we chose. The admittance is found to be

$$y_{\rm Re}=(e^2m/2\pi^2\hbar^3)T_{0,\max}\Gamma\frac{\Gamma}{4\hbar\omega(4\Gamma^2+\hbar^2\omega^2)}\Bigg[4\Gamma\hbar\omega\left(\tan^{-1}\frac{E_F-E_R}{\Gamma}+\tan^{-1}\frac{E_R}{\Gamma}\right)$$
$$+4\Gamma(E_F-E_R+\hbar\omega/2)\left(\tan^{-1}\frac{E_F-E_R+\hbar\omega}{\Gamma}+\tan^{-1}\frac{E_R-\hbar\omega}{\Gamma}\right)$$
$$-4\Gamma(E_F-E_R-\hbar\omega/2)\left(\tan^{-1}\frac{E_F-E_R-\hbar\omega}{\Gamma}+\tan^{-1}\frac{E_R+\hbar\omega}{\Gamma}\right)$$
$$+2\hbar\omega(E_F-E_R)\ln\frac{(E_F-E_R)^2+\Gamma^2}{E_R^2+\Gamma^2}$$
$$-[\hbar\omega(E_F-E_R-\hbar\omega)-2\Gamma^2]\ln\frac{(E_F-E_R-\hbar\omega)^2+\Gamma^2}{(E_R+\hbar\omega)^2+\Gamma^2}$$
$$-[\hbar\omega(E_F-E_R+\hbar\omega)+2\Gamma^2]\ln\frac{(E_F-E_R+\hbar\omega)^2+\Gamma^2}{(E_R-\hbar\omega)^2+\Gamma^2}\Bigg], \tag{26}$$

$$
\begin{aligned}
y_{\mathrm{Im}} = {} & (e^2 m/2\pi^2\hbar^3) T_{0,\max}\Gamma \frac{\Gamma}{2\hbar\omega(4\Gamma^2+\hbar^2\omega^2)} \\
& \times \Bigg[-4\Gamma^2 \left(\tan^{-1}\frac{E_F - E_R}{\Gamma} + \tan^{-1}\frac{E_R}{\Gamma} \right) \\
& + [\hbar\omega(E_F - E_R + \hbar\omega) + 2\Gamma^2] \left(\tan^{-1}\frac{E_F - E_R + \hbar\omega}{\Gamma} + \tan^{-1}\frac{E_R - \hbar\omega}{\Gamma} \right) \\
& - [\hbar\omega(E_F - E_R - \hbar\omega) - 2\Gamma^2] \left(\tan^{-1}\frac{E_F - E_R - \hbar\omega}{\Gamma} + \tan^{-1}\frac{E_R + \hbar\omega}{\Gamma} \right) \\
& - 2\Gamma(E_F - E_R)\ln\frac{(E_F - E_R)^2 + \Gamma^2}{E_R^2 + \Gamma^2} + \Gamma(E_F - E_R - \hbar\omega/2)\ln\frac{(E_F - E_R - \hbar\omega)^2 + \Gamma^2}{(E_R + \hbar\omega)^2 + \Gamma^2} \\
& + \Gamma(E_F - E_R + \hbar\omega/2)\ln\frac{(E_F - E_R + \hbar\omega)^2 + \Gamma^2}{(E_R - \hbar\omega)^2 + \Gamma^2} \Bigg] . \qquad (27)
\end{aligned}
$$

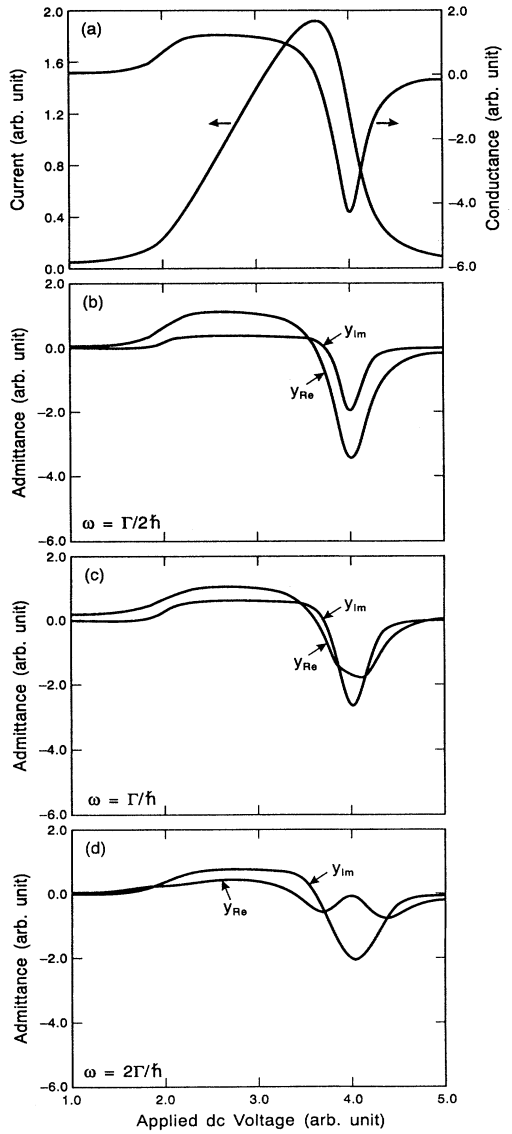

FIG. 3. (a) dc current-voltage (I-V) and dI/dV-V characteristics; (b), (c), and (d) Real and imaginary parts of the device admittance for $\hbar\omega = \Gamma/2, \Gamma$, and 2Γ, respectively.

Figure 3 plots (a) a dc I-V and dI/dV-V characteristics using Eq. (17), (b), (c), and (d) the device admittances for $\hbar\omega = \Gamma/2, \Gamma$, and 2Γ, respectively. We have adopted an arbitrary unit system in which we set $E_F = 1, E_{R0} = 2$, and $\Gamma = \frac{1}{10}$. For example, we omit the factor $(em/2\pi^2\hbar^3)T_{0,\max}\Gamma$ in Eq. (17) and plot the rest in the above unit system. From Fig. 3 the real part of the admittance follows the dI/dV-V curve for low frequencies $\hbar\omega < \Gamma$, and in fact it is identical to dI/dV-V in the limit $\hbar\omega \ll \Gamma$ as we have shown explicitly in Eq. (23). The imaginary part has the general shape of dI/dV for low frequencies but increases with $\hbar\omega$ roughly linearly. This behavior is intuitively expected from Eq. (23). The real part and the shape of the imaginary part of the device admittance deviate from the dc dI/dV-V curve in high frequencies $\hbar\omega > \Gamma$. Physically this is because for $\hbar\omega > \Gamma$ the time scale involved in RT is relatively long

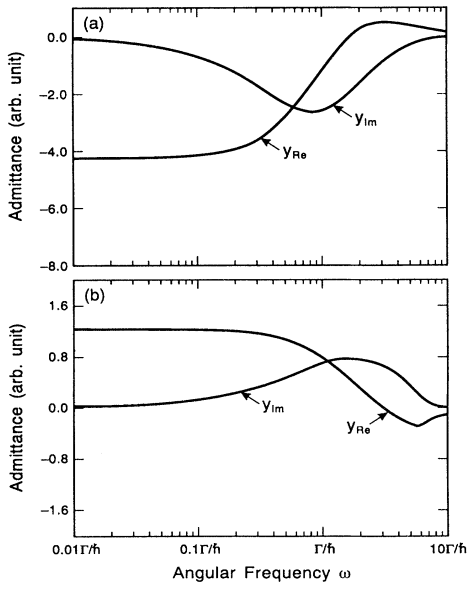

FIG. 4. (a) and (b) Real and imaginary parts of the device admittance vs ω in the negative and the positive differential resistance regions, respectively.

compared with the frequency of the applied ac voltage and the electrons can no longer follow the instantaneous change of the potential as a function of time. Figure 4 plots the device admittance versus frequency for (a) a dc bias voltage of 4.0 which corresponds to a dc bias point in the NDR region, and for (b) a bias of 2.8 which is in the positive resistance region of the I-V [see Fig. 3(a)]. The horizontal axis is scaled by $\Gamma/\hbar$. The behavior shown in Fig. 4 is very similar to previous reported results using numerical calculations.[28,29]

IV. PHOTON EMISSION EFFICIENCY

In this section we consider the net number of photons emitted into the ac field by counting the difference between the number of electrons which undergo the t_{-1} (emission) process and the number for t_{+1} process. Consider the following current difference:

$$\Delta j = j_{-1} - j_{+1} = (e\hbar k/m)(T_{-1} - T_{+1}), \tag{28}$$

which represents the net current (not directly observable) associated with photon emission. Let us first consider the Taylor series expansion of the leading term of the quantity $\Delta T \equiv T_{-1} - T_{+1}$ with respect to $\hbar\omega$ using Eq. (7):

$$\Delta T = (V_{\rm ac}/2\hbar\omega)^2 T_0 \frac{2\hbar\omega(E - E_R)}{(E - E_R)^2 + \Gamma^2} - O((\hbar\omega)^2)$$
$$= -(V_{\rm ac}^2/2\hbar\omega)(\partial T_0/\partial V_{\rm dc}) - O((\hbar\omega)^2).$$

Substituting the above into Eq. (28) then (15) we get the total current difference ΔJ. Multiplying ΔJ by $\hbar\omega/e$ we get the net photon power ΔP (joules per unit time per unit area):

$$\Delta P = -0.5(V_{\rm ac}/e)^2 \frac{\partial J_{\rm dc}}{\partial(V_{\rm dc}/e)} - O((\hbar\omega)^2). \tag{29}$$

It is clear that only in the NDR region where $\partial J_{\rm dc}/\partial V_{\rm dc} < 0$ can there be a net photon output. Equation (29) represents a low-frequency expansion.

For arbitrary frequencies, we use the full expression [Eq. (7)] and substitute Eq. (28) into (15). The integration over the Fermi sea leads to an expression similar to Eqs. (26) and (27). Figure 5 shows the net power versus ω for the device parameters as in Fig. 3 using the same arbitrary unit system, and for a fixed $V_{\rm ac}$ and an applied dc bias of 4.0 which is in the NDR region. Note that the emission that we consider here originates from the RT structure itself, and other considerations must be made if a RT oscillator is connected to an antenna.

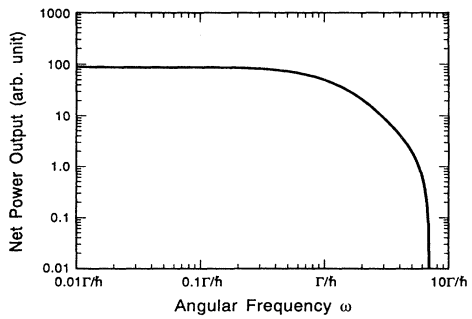

FIG. 5. Net power output emitted into the ac field vs frequency when a device is biased in the negative differential resistance region.

V. CONCLUDING REMARKS

To conclude, we have presented an analytical model for high-frequency resonant tunneling. A scattering theory approach has been used, and analytical results for transmission coefficients and tunneling current have been derived. The ac tunneling current shows a phase delay relative to the applied voltage due to the finite lifetime of the resonant state, and starts to deviate from the classical result when $\hbar\omega$ approaches Γ. Our model is valid so long as the applied electromagnetic field can be described by a voltage. For higher frequencies where the wavelength of the electromagnetic field in the material is comparable or smaller than the geometrical size of the device, a full quantum-mechanical description should be employed. Electromagnetic waves in the double-barrier region should be described by photon fields. A perturbative approach has been given for single-barrier tunneling.[30] The same formalisms could be used for a double-barrier structure in the presence of a photon field. Our model can be also used together with the results calculated including self-consistency between the Schrödinger equation and the Poisson equation for the static case[16–18] because the inputs to our model are characteristic parameters like the resonance width, the on-resonance transmission, the resonance energy, and the Fermi energy in the emitter. This makes the model useful in practical devices. Further theoretical work includes (a) searching for an analytical result for the second-order sidebands which will enable us to calculate the rectification (dc detection) coefficient,[1] the second harmonic coefficient, and so on; (b) incorporating charge effects on the potential profile which will have device intrinsic capacitive effects included in the model; and (c) including scattering effects such as by impurities in the double barrier, interface roughness, and phonons.

ACKNOWLEDGMENTS

The author benefited from discussions with Dr. E. R. Brown, Dr. P. J. Price, and Dr. T. C. L. G. Sollner, and would like to thank Dr. G. C. Aers for many discussions one of which led to the derivation in Appendix C.

APPENDIX A: REVIEW OF THE BASIC APPROACH

We briefly review a method[14,15] which can be used to solve a general potential profile in the presence of both dc and ac voltages, and, in the process, the form of the wave function in Eq. (4) will be justified. The approach that we

use here is as follows: given an arbitrary potential profile, one can always approximate to an arbitrary accuracy the actual profile by a series of steps, i.e., divide the space into regions with constant potentials. The problem then reduces to (a) finding a general solution for a spatially constant potential $v_{dc} + v_{ac}\cos\omega t$ where v_{dc} and v_{ac} are constants; and (b) matching solutions in adjacent regions with different values of v_{dc} and v_{ac}.

Analogous to the 2×2 transfer matrix approach for the dc case,[12,13] we first find plane-wave-like solutions to the time-*dependent* Schrödinger equation

$$i\hbar\frac{\partial\psi}{\partial t} = -\frac{\hbar^2}{2m}\frac{\partial^2\psi}{\partial z^2} + (v_{dc} + v_{ac}\cos\omega t)\psi, \tag{A1}$$

for constant v_{dc} and v_{ac}. One can easily verify that the following is a solution:

$$\psi_k = e^{ikz - iEt/\hbar - i(v_{ac}/\hbar\omega)\sin\omega t}, \tag{A2}$$

where $E - v_{dc} = \hbar^2k^2/2m$. The above describes a plane wave with energy E and wave vector k. We then construct a general solution with energy components $E+n\hbar\omega$ $(n = 0, \pm1, \pm2, \ldots)$:

$$\psi = \sum_n (a_n\psi_{k_n} + b_n\psi_{-k_n}), \tag{A3}$$

where $E + n\hbar\omega - v_{dc} = \hbar^2k_n^2/2m$. Note that within a constant potential region there are no mixings between plane waves with different energies, and mixings (radiative transitions) occur at an ac potential step (and are described by the following transfer matrix). This physically is equivalent to transitions induced by a spatially varying (linear in our case) time-dependent ($\cos\omega t$ in our case) potential. If the solution in the next constant potential region is written as $\psi' = \sum_n (c_n\psi_{k'_n} + d_n\psi_{-k'_n})$, we require a general transfer matrix M so that $(c,d)^T = M(a,b)^T$, where $a = (\ldots, a_2, a_1, a_0, a_{-1}, a_{-2}, \ldots)$, similarly for b, c, and d, and the superscript T means transposing the row matrix. Assuming the simplest boundary conditions, ψ and $\partial\psi/\partial z$ continuous, we find[14]

$$M = \frac{1}{2}\begin{pmatrix} (\xi)_+ & (\xi)_- \\ (\xi)_- & (\xi)_+ \end{pmatrix}, \tag{A4}$$

$$(\xi)_\pm = \begin{pmatrix} & \vdots & & & \\ \cdots & \xi^{(0)}_{1,1} & \xi^{(1)}_{1,0} & \xi^{(2)}_{1,-1} & \cdots \\ \cdots & \xi^{(-1)}_{0,1} & \xi^{(0)}_{0,0} & \xi^{(1)}_{0,-1} & \cdots \\ \cdots & \xi^{(-2)}_{-1,1} & \xi^{(-1)}_{-1,0} & \xi^{(0)}_{-1,-1} & \cdots \\ & \vdots & & & \end{pmatrix}, \tag{A5}$$

where $\xi^{(p)}_{qr} = J_p(\Delta v_{ac}/\hbar\omega)(1 \pm k_r/k'_q)$, $\Delta v_{ac} = v'_{ac} - v_{ac}$, and J_p is the integer Bessel function. In general, the effective mass m in different regions can be different, and using physical arguments for the envelope wave function, one requires continuities of ψ and $(1/m)\partial\psi/\partial z$. However, such boundary conditions complicate the one-dimensional model because energies associated with x, y, and z direction motions are no longer individually conserved. To continue onto the next potential step, one must first multiply the matrix by a diagonal propagation matrix M' which is equivalent to moving the coordinate origin to coincide with the next potential discontinuity. The diagonal elements of M' are $(\ldots, e^{ik'_{+1}d'}, e^{ik'_0d'}, e^{ik'_{-1}d'}, \ldots, e^{-ik'_{+1}d'}, e^{-ik'_0d'}, e^{-ik'_{-1}d'}, \ldots)$, where d' is the length of the region. Multiplying M' and M together for all the potential steps, we obtain the transfer matrix to relate constants a and b on one side of the structure to c and d on the other side. Transmission and reflection amplitudes for an incident electron with energy E are found by setting $a = (\ldots, 0, 0, 1, 0, 0, \ldots)$, $b = (\ldots, r_2, r_1, r_0, r_{-1}, r_{-2}, \ldots)$, $c = (\ldots, t_2, t_1, t_0, t_{-1}, t_{-2}, \ldots)$, and $d = (\ldots, 0, 0, 0, 0, 0, \ldots)$. Then a multichannel scattering state consists of the incident wave [Eq. (3)], and the scattered (transmitted and reflected) waves. Equation (4) shows the transmitted waves including only up to $n = \pm1$ sidebands.

As an example of how the t_n and r_n are determined, let us consider a potential discontinuity with an ac step only, i.e., $v_{dc} = v'_{dc}$ and $v_{ac} \neq v'_{ac}$, and include only the first-order sidebands. The transfer matrix becomes 6×6, and for $E \gg \hbar\omega$:

$$M \approx \begin{pmatrix} J_0 & J_1 & 0 & & & \\ J_{-1} & J_0 & J_1 & 0 & & \\ 0 & J_{-1} & J_0 & & & \\ & & & J_0 & J_1 & 0 \\ & 0 & & J_{-1} & J_0 & J_1 \\ & & & 0 & J_{-1} & J_0 \end{pmatrix}, \tag{A6}$$

where the Bessel functions are $J_{0,\pm1}(\Delta v_{ac}/\hbar\omega)$. Transmission and reflection amplitudes for such a simple case are determined: $t_{0,\pm1} \approx J_{0,\pm1}(\Delta v_{ac}/\hbar\omega)$ and $r_{0,\pm1} \approx 0$. This result will be used in Appendix C. The physical meaning of quantities $t_{\pm1}$ here are that they are the absorption $(+1)$ and emission (-1) matrix elements of one ac modulation quantum $\hbar\omega$ for an electron crossing an ac potential step.

APPENDIX B: DERIVATION OF DIRECT TUNNELING AMPLITUDE

We give two methods to derive the direct tunneling amplitude t_0. First, we briefly review the derivation in a ray-tracing (Fabry-Perot) scheme.[31] Suppose the transmission amplitudes for the emitter barrier and the collector barrier in the direction of the current flow are t_E and t_C, the reflection amplitudes off the interfaces defining the quantum well are r_E and r_C, respectively, the wave vector in the well is q, and the well width is w. Summing over all possible paths, we get

$$\begin{aligned} t_0 &= t_E\tilde{e}t_C + t_E\tilde{e}(r_Cr_E\tilde{e}^2)t_C + t_E\tilde{e}(r_Cr_E\tilde{e}^2)^2t_C + \cdots \\ &= \frac{t_Et_C\tilde{e}}{1 - \tilde{e}^2r_Er_C}, \end{aligned} \tag{B1}$$

where $\tilde{e} \equiv \exp(iqw)$ or $\exp(\int_0^w iq\,dw)$ if there exists an electric field in the well. A resonance occurs when the

phase of the complex quantity $\tilde{e}^2 r_C r_E$ equals an integer times 2π, i.e., $\tilde{e}^2 r_C r_E = |r_C r_E|$, and the corresponding energy is E_R. The current conservation gives $|r_C|^2 + (k_0/q)|t_C|^2 = 1$ and $|r_E|^2 + (q/k)|t_E|^2 = 1$. We have used the fact that the magnitudes of reflection amplitudes are independent of the incident directions which can be shown easily from the unitarity relation of the scattering matrix.[13] We define the transmission coefficients as $T_E = (q/k)|t_E|^2$ and $T_C = (k_0/q)|t_C|^2$. For $|r_E|$ and $|r_C|$ close to unity, we have $|r_E| \approx 1 - T_E/2$ and $|r_C| \approx 1 - T_C/2$. From Eq. (B1) we then have the on-resonance (maximum) transmission coefficient for the entire structure at $E = E_R$,

$$T_{0,\max} = \frac{k_0}{k}|t_0|^2_{\max} \approx \frac{4T_E T_C}{(T_E + T_C)^2}. \tag{B2}$$

Note that when $T_E = T_C$, $T_{0,\max} = 1$ is rigorous.

We express the denominator in Eq. (B1) in the following way and expand the phase to the first order in the neighborhood of E_R:

$$1 - |r_E r_C| e^{i\theta} \approx (T_E + T_C)/2 - i\theta'|_{E_R}(E - E_R), \tag{B3}$$

where θ' is $\partial\theta/\partial E$. Then the transmission amplitude is

$$t_0 \approx \frac{2t_E t_C \tilde{e}}{T_E + T_C} \frac{i\Gamma}{E - E_R + i\Gamma}, \tag{B4}$$

where the resonance width $\Gamma = (T_E + T_C)/2\theta'|_{E_R}$. The transmission coefficient $T_0 = (k_0/k)|t_0|^2$, and the phase (ϕ_0) of t_0 are then

$$T_0 \approx T_{0,\max} \frac{\Gamma^2}{(E - E_R)^2 + \Gamma^2}, \tag{B5}$$

$$\phi_0 \approx \phi_{00} + \tan^{-1}\frac{E - E_R}{\Gamma}, \tag{B6}$$

where ϕ_{00} is the phase of $t_E t_C \tilde{e}$. The phase change across a resonance (i.e., from $E \ll E_R$ to $E \gg E_R$) amounts to π which has been pointed out to be true in general by Wigner.[32]

The second method that we use to derive the expression for t_0 is by the transfer matrix which connects two independent plane waves from one constant potential region to another region.[12,13] We start the matrix matching from the *emitter* side to the *collector* side. The transfer matrices for the emitter and the collector barriers are

$$\begin{pmatrix} t_E - r_E r'_E/t'_E & r_E/t'_E \\ -r'_E/t'_E & 1/t'_E \end{pmatrix}, \tag{B7}$$

$$\begin{pmatrix} t_C - r_C r'_C/t'_C & r'_C/t'_C \\ -r_C/t'_C & 1/t'_C \end{pmatrix}, \tag{B8}$$

where the primed quantities are the same as the corresponding unprimed except the electron traveling directions are reversed, e.g., t'_C is the transmission amplitude for an electron incident from the collector side. Multiplying matrices (B7) and (B8) together with a plane-wave propagation in the well, we get the total transfer matrix (M) for the double barrier

$$M = \begin{pmatrix} t_C - r_C r'_C/t'_C & r'_C/t'_C \\ -r_C/t'_C & 1/t'_C \end{pmatrix} \begin{pmatrix} \tilde{e} & 0 \\ 0 & \tilde{e}^{-1} \end{pmatrix} \times \begin{pmatrix} t_E - r_E r'_E/t'_E & r_E/t'_E \\ -r'_E/t'_E & 1/t'_E \end{pmatrix}. \tag{B9}$$

The element $(M)_{22}$ is the inverse of the transmission amplitude for an electron incident from the *collector*. Interchanging primed and unprimed quantities, we obtain

$$t_0 = \frac{t_E t_C \tilde{e}}{1 - \tilde{e}^2 r_E r_C}, \tag{B10}$$

which is identical to Eq. (B1), and hence, a Breit-Wigner expansion in the neighborhood of the resonance leads to Eqs. (B5) and (B6).

We stress that the Fabry-Perot derivation for a RT electron is only analogous to a particle "bouncing back and forth" in the well because of the wave nature of the Schrödinger equation. Strictly speaking this does not mean that the electron motion follows such a path. As we see from the second derivation that the RT phenomenon only needs the existence of the resonant quasibound state.[19]

APPENDIX C: DERIVATION OF FIRST-ORDER SIDEBANDS

We approximate the spatially linear potential by a series of steps and then let the number of the steps go to infinity. We first illustrate our method by considering a special case where the absorption or emission occurs at the center of the well. We use the following simplified notations: symbols with superscripts $*$ have the same meanings but evaluated at an energy higher or lower by $\hbar\omega$, $\mathcal{M}$ is the emission $(\mathcal{M}_{-1})$ or absorption $(\mathcal{M}_{+1})$ matrix element, and $\tilde{e}_{1/2} \equiv \tilde{e}^{1/2} \equiv \exp(iqw/2)$ is a phase term corresponding to propagation halfway across the well. The possible paths are

$$\begin{aligned} t_{\pm 1} = {} & t_E \tilde{e}_{1/2} \mathcal{M} \tilde{e}^*_{1/2} t^*_C + t_E \tilde{e} r_C \tilde{e} r_E \tilde{e}_{1/2} \mathcal{M} \tilde{e}^*_{1/2} t^*_C \\ & + t_E \tilde{e} r_C \tilde{e}_{1/2} (-\mathcal{M}) \tilde{e}^*_{1/2} r^*_E \tilde{e}^* t^*_C \\ & + t_E \tilde{e}_{1/2} \mathcal{M} \tilde{e}^*_{1/2} r^*_C \tilde{e}^* r^*_E \tilde{e}^* t^*_C + \cdots, \end{aligned} \tag{C1}$$

where the reason for the minus sign in $(-\mathcal{M})$ of the third term will be given below. After carrying out the summation, we get

$$t_{\pm 1} = \frac{t_E \tilde{e}_{1/2} \mathcal{M} \tilde{e}^*_{1/2} t^*_C (1 - \tilde{e}\tilde{e}^* r^*_E r_C)}{(1 - \tilde{e}^2 r_E r_C)(1 - \tilde{e}^{*2} r^*_E r^*_C)}. \tag{C2}$$

The summation can be easily seen diagrammatically. Figure 6 shows the leading terms for t_{+1} and the four terms in Eq. (C1) correspond to the first two rows in the figure. If we continue the figure, each row will have two more terms. Columns can be summed up and the resulting expression can be summed up again leading to the

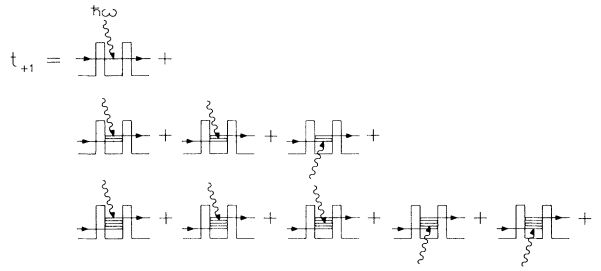

FIG. 6. Diagrammatic representation of possible paths of the first-order absorption sideband t_{+1} when the absorption occurs in the well.

result in Eq. (C2). The matrix element $\mathcal{M}_{\pm1}$ is calculated using the technique developed early[14,26] as given in Appendix A and it is essentially the transmission amplitudes through an ac potential step $-\Delta V_{\rm ac}\cos\omega t$:

$$\mathcal{M}_{\pm1} \approx J_{\pm1}(-\Delta V_{\rm ac}/\hbar\omega) \approx \mp\Delta V_{\rm ac}/2\hbar\omega. \tag{C3}$$

We have expanded the Bessel functions $J_{\pm1}(\cdots)$, therefore the above holds for $\Delta V_{\rm ac}/\hbar\omega \ll 1$. If we reverse the electron traveling direction, the matrix element $\mathcal{M}$ changes to $-\mathcal{M}$ which is the reason for the minus sign in $(-\mathcal{M})$ of the third term in Eq. (C1). Equation (C2) holds for all cases where the emission or absorption occur at a given position within the *well* (with an appropriate change in $\tilde{e}_{1/2}$, $\tilde{e}^*_{1/2}$, $\tilde{e}$, and $\tilde{e}^*$). Specifically, let x be the fraction of the well width at which the interaction occurs $0 < x < 1$, e.g., Eqs. (C1) and (C2) correspond to $x = \frac{1}{2}$. Equation (C2) becomes

$$t_{\pm1} = \frac{t_E\tilde{e}_x\mathcal{M}\tilde{e}^*_{1-x}t^*_C(1-\tilde{e}^2_{1-x}\tilde{e}^{*2}_x r^*_E r_C)}{(1-\tilde{e}^2 r_E r_C)(1-\tilde{e}^{*2}r^*_E r^*_C)}. \tag{C4}$$

In general, the ac voltage across the *well* is linearly distributed which can be approximated to an arbitrary accuracy by a series of steps. Since Eq. (C4) is linear in $\mathcal{M}$ and $\mathcal{M}$ is proportional to $\Delta V_{\rm ac}$, an integration of Eq. (C4) with respect to x from $x = 0$ to $x = 1$ corresponds to distributing the ac voltage linearly across the well. Note that $\tilde{e}_x\tilde{e}^*_{1-x}\tilde{e}_{1-x}\tilde{e}^*_x = \tilde{e}\tilde{e}^*$. We then need to consider only the integrations for terms $\tilde{e}_x\tilde{e}^*_{1-x}$ and $\tilde{e}_{1-x}\tilde{e}^*_x$ which give

$$\int_0^1 \tilde{e}_x\tilde{e}^*_{1-x}dx = \int_0^1 \tilde{e}_{1-x}\tilde{e}^*_x dx = \frac{\exp(iqw)-\exp(iq^*w)}{i(q-q^*)w}. \tag{C5}$$

If we assume that the kinetic energy of the electron in the well is much larger than $\hbar\omega$, i.e., the incident electron energy referenced to the well band edge is much larger than $\hbar\omega$. The final result in Eq. (C5) can be approximated:

$$\frac{\exp(iqw)-\exp(iq^*w)}{i(q-q^*)w} \approx \tilde{e}_{1/2}\tilde{e}^*_{1/2}. \tag{C6}$$

This shows that Eq. (C2) is valid even when the voltage across the well is linearly distributed, i.e., for the portion of the ac voltage in the well the first-order sidebands are given by Eq. (C2) with $\Delta V_{\rm ac}$ in Eq. (C3) corresponding to the ac potential across the entire well.

For the portion of the ac voltage in the barriers, we illustrate the derivation briefly without going through the details. Equation (C3) holds in both classically allowed and forbidden regions as long as the electron energy is well separated from the band edge. Figure 7 shows schematically the physical processes. For an equal barrier width structure, i.e., the amounts of the ac potentials across the emitter and the collector barriers are the same, the first-order sidebands due to ac potentials in the barriers are

$$\begin{aligned} t_{\pm1} &\approx \frac{t_E t^*_C\tilde{e}^*\mathcal{M}}{1-\tilde{e}^{*2}r^*_E r^*_C} + \frac{t_E t^*_C\tilde{e}\mathcal{M}}{1-\tilde{e}^2 r_E r_C} \\ &= t_E t^*_C\mathcal{M}\frac{\tilde{e}^*(1-\tilde{e}^2 r_E r_C)+\tilde{e}^*(1-\tilde{e}^{*2}r^*_E r^*_C)}{(1-\tilde{e}^2 r_E r_C)(1-\tilde{e}^{*2}r^*_E r^*_C)}, \end{aligned} \tag{C7}$$

where we have assumed that in the barriers the separation between the band edge (barrier height) and the electron energy is much larger than $\hbar\omega$. In the above equation $\Delta V_{\rm ac}$ which appears in $\mathcal{M}$ corresponds to the potential across one barrier. Terms in parentheses in Eqs. (C2) and (C7) are very similar or identical to the denominator in Eq. (B1), and hence we can make a similar expansion in the neighborhood of the resonance and then add the two contributions [Eqs. (C2) and (C7)] together:

$$t_{\pm1} \approx \frac{2t_E t_C\tilde{e}}{T_E+T_C}\frac{\mathcal{M}_{\pm1}i\Gamma(E-E_R\pm\hbar\omega/2+i\Gamma)}{(E-E_R\pm\hbar\omega/2+i\Gamma)(E-E_R+i\Gamma)}, \tag{C8}$$

where $\Delta V_{\rm ac}$ in $\mathcal{M}$ is now the total potential $V_{\rm ac}$. The transmission coefficients, and the phases $(\phi_{\pm1})$ of $t_{\pm1}$ are then

$$\begin{aligned} T_{\pm1} &\approx |\mathcal{M}_{\pm1}|^2 T_{0,\max} \\ &\quad\times\frac{\Gamma^2[(E-E_R\pm\hbar\omega/2)^2+\Gamma^2]}{[(E-E_R)^2+\Gamma^2][(E-E_R\pm\hbar\omega)^2+\Gamma^2]}, \end{aligned} \tag{C9}$$

$$\begin{aligned} \phi_{\pm1} &\approx \phi_{\pm1,0} + \tan^{-1}\frac{E-E_R}{\Gamma} - \tan^{-1}\frac{E-E_R\pm\hbar\omega/2}{\Gamma} \\ &\quad + \tan^{-1}\frac{E-E_R\pm\hbar\omega}{\Gamma}, \end{aligned} \tag{C10}$$

where $\phi_{+1,0} \approx \phi_{00}$ and $\phi_{-1,0} \approx \phi_{00}+\pi$. Note that the above approximation becomes worse when $\hbar\omega$ is much larger than Γ because the Breit-Wigner-like expansion fails far away from the resonance. The phase change for $t_{\pm1}$ from $E \ll E_R$ to $E \gg E_R$ is again π.

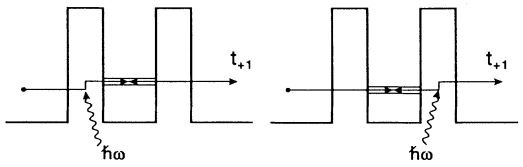

FIG. 7. Diagrammatic representation of the first-order absorption sideband t_{+1} when the absorption occurs in the emitter (left part) and collector (right part) barriers.

[1]T. C. L. G. Sollner, W. D. Goodhue, P. E. Tannenwald, C. D. Parker, and D. D. Peck, Appl. Phys. Lett. **43**, 588 (1983).
[2]E. R. Brown, T. C. L. G. Sollner, W. D. Goodhue, and C. D. Parker, Appl. Phys. Lett. **50**, 83 (1987).
[3]T. C. L. G. Sollner, E. R. Brown, W. D. Goodhue, and H. Q. Le, Appl. Phys. Lett. **50**, 332 (1987).
[4]E. R. Brown, C. D. Parker, and T. C. L. G. Sollner, Appl. Phys. Lett. **54**, 934 (1989).
[5]E. R. Brown, T. C. L. G. Sollner, C. D. Parker, W. D. Goodhue, and C. L. Chen, Appl. Phys. Lett. **55**, 1777 (1989).
[6]F. Capasso, S. Sen, A. C. Gossard, A. L. Hutchinson, and J. H. English, IEEE Electron Device Lett. **EDL-7**, 573 (1986).
[7]M. A. Reed, W. R. Frensley, R. J. Matyi, J. N. Randall, and A. C. Seabaugh, Appl. Phys. Lett. **54**, 1034 (1989).
[8]J. F. Young, B. W. Wood, H. C. Liu, M. Buchanan, D. Landheer, A. J. SpringThorpe, and P. Mandeville, Appl. Phys. Lett. **52**, 1389 (1988).
[9]V. J. Goldman, D. C. Tsui, and J. E. Cunningham, Phys. Rev. Lett. **58**, 1256 (1987); T. C. L. G. Sollner, *ibid.* **59**, 1622 (1987).
[10]M. Tsuchiya, T. Matsusue, and H. Sakaki, Phys. Rev. Lett. **59**, 2356 (1987).
[11]J. F. Young, B. W. Wood, G. C. Aers, R. L. S. Devine, H. C. Liu, D. Landheer, M. Buchanan, A. J. SpringThorpe, and P. Mandeville, Phys. Rev. Lett. **60**, 2058 (1988).
[12]R. Tsu and L. Esaki, Appl. Phys. Lett. **22**, 562 (1973).
[13]D. D. Coon and H. C. Liu, Appl. Phys. Lett. **47**, 172 (1985).
[14]D. D. Coon and H. C. Liu, J. Appl. Phys. **58**, 2230 (1985).
[15]D. D. Coon and H. C. Liu, Solid State Commun. **55**, 339 (1985).
[16]H. Ohnishi, T. Inata, S. Muto, N. Yokoyama, and A. Shibatomi, Appl. Phys. Lett. **49**, 1248 (1986).
[17]M. Cahay, M. McLennan, S. Datta, and M. S. Lundstrom, Appl. Phys. Lett. **50**, 612 (1987).
[18]T. Baba and M. Mizuta, Jpn. J. Appl. Phys. **28**, L1322 (1989).
[19]S. Luryi, Appl. Phys. Lett. **47**, 490 (1985).
[20]D. D. Coon and H. C. Liu, Appl. Phys. Lett. **49**, 94 (1986).
[21]S. C. Kan and A. Yariv, J. Appl. Phys. **64**, 3098 (1988).
[22]W. R. Frensley, Phys. Rev. Lett. **57**, 2853 (1986).
[23]W. R. Frensley, Phys. Rev. B **36**, 1570 (1987); **37**, 10 379 (1988).
[24]C. Jacoboni and P. J. Price, Solid State Commun. **75**, 193 (1990).
[25]M. Büttiker and R. Landauer, Phys. Rev. Lett. **49**, 1739 (1983).
[26]H. C. Liu, Appl. Phys. Lett. **52**, 483 (1988).
[27]A. Tackeuchi, T. Inata, S. Muto, and E. Miyauchi, Jpn. J. Appl. Phys. **28**, L750 (1989).
[28]W. R. Frensley, Appl. Phys. Lett. **51**, 448 (1987).
[29]R. K. Mains and G. I. Haddad, J. Appl. Phys. **64**, 3564 (1988).
[30]D. D. Coon and H. C. Liu, Solid State Commun. **54**, 275 (1985).
[31]M. Jonson and A. Grincwajg, Appl. Phys. Lett. **51**, 1729 (1987).
[32]E. P. Wigner, Phys. Rev. **98**, 145 (1955).